IEEE Access
Multidisciplinary ⋮ Rapid Review ⋮ Open Access Journal

Received August 12, 2019, accepted September 1, 2019, date of publication September 13, 2019, date of current version October 7, 2019.

Digital Object Identifier 10.1109/ACCESS.2019.2940974

Command Filtered Model-Free Robust Control for Aircrafts With Actuator Dynamics

XIAOFENG LI[1], LIJIA CAO[2,3,4], XIAOXIANG HU[5], AND SHENGXIU ZHANG[1]

[1]Xi'an Research Institute of Hi-Tech, Xi'an 710025, China
[2]Artificial Intelligence Key Laboratory of Sichuan Province, Zigong 643000, China
[3]School of Automation and Information Engineering, Sichuan University of Science and Engineering, Zigong 643000, China
[4]Sichuan Key Provincial Research Base of Intelligent Tourism, Zigong 643000, China
[5]School of Automation, Northwestern Polytechnical University, Xi'an 710068, China

Corresponding author: Lijia Cao (caolj@suse.edu.cn)

This work was supported in part by the National Science Foundation of China under Grant 61773387 and Grant 61703409, in part by the Aeronautical Science Foundation of China under Grant 201605U8002, in part by the Sichuan Science and Technology Program under Grant 19ZDZX0037, in part by the Nature Science Foundation of Sichuan University of Science and Engineering under Grant 2018RCL18, and in part by the Sichuan Key Provincial Research Base of Intelligent Tourism under Grant ZHZJ18-01.

ABSTRACT In this paper, a command filtered model-free robust (CFMFR) controller is proposed to regulate attitude angles of an aircraft with parameter uncertainties and disturbances to track the given reference signals. For the first subsystem of the controlled plant, the incremental nonlinear dynamic inversion (INDI) is applied to design incremental virtual control law. While the time-delayed control (TDC) method is used to design the control law by integrating sliding-mode technique considering the nominal value of the control effectiveness matrix is unknown. The adaption laws of the control gain are constructed by Lyapunov control theorem. Not only the actuator dynamics of the control surfaces are considered, but also the noises, biases, and time delays of the measurements of the control surface deflection angles are taken into account. Therefore, the command-filtered backstepping is utilized to compensate for the actuator dynamics and filtered errors, and the modified stable linear filter is developed to handle the measurement errors. The stability of the whole closed-loop system, including the compensated signals which are the outputs of the stable linear filters, is analyzed by using Lyapunov theory. The numerical simulation results demonstrate effectiveness of the proposed CFMFR control approach with updating matrix.

INDEX TERMS Unmanned aerial vehicles, attitude control, command filter technique, backstepping control method.

I. INTRODUCTION

Backstepping control method [1] is proposed by I. Kanellakopoulos, P.V. Kokotovic, and A.S. Morse in 1991. It has been widely applied to variable applications, such as motors [2], aircrafts [3], robots [4], and so on. As for the traditional backstepping control method, there are two main drawbacks: (1) complicated calculation of partial derivatives are necessary, which may cause 'explosion of complexity' as the orders of the controlled plant increase; (2) the concrete mathematical model must be known. With respect to the first drawback, the dynamic surface control (DSC) [5] and command filter technique [6]–[8] all have been successfully applied to make the control laws more concise. They all make full use of the filters to obtain the derivatives of the virtual control laws. Note that the command filter with magnitude, rate, and bandwidth limitations proposed in [6] can ensure that the command trajectory and its derivative meet the magnitude and rate constraints to meet the states and actuator physical constraints. The second drawback also attracted many scholars' attention for that robustness of the traditional backstepping is questioned in the real practice. It is nearly impossible to construct the precise mathematical model for a controlled plant under the existence of the uncertainties and disturbances. The disturbance observers [9], [10] are used to identify the unknown disturbances and uncertain parameters to improve the robustness of the controller with the condition that the nominal value of the mathematical model of the system is prior known. The neural network (NN) [11] and fuzzy logic system (FLS) [8], [12]

The associate editor coordinating the review of this manuscript and approving it for publication was Xiaoli Luan.

are also employed to identify the uncertain or even unknown functions of the system whereas the calculation complexity would be increased significantly for that large numbers of parameters should be identified on-line.

Incremental nonlinear dynamic inversion (INDI) [13], [14], which is a kind of sensor-based control method [15], [16], transformed the dynamics of the system into a sum of the first derivative of the state in the last sampling time and a product term including the incremental input and the control effectiveness matrix. The first derivatives of the states can reflect the changes and information of the complicated mathematical model. In [17], the INDI method is applied to design the virtual control laws for each subsystem. There is an assumption here that the nominal value of the control matrices is known. To handle the uncertainties in the control effectiveness matrix, techniques involving tuning functions [18], the least-squares method [19], and immersion and invariance [20] have been applied to the estimator design, and these estimators were evaluated in [21]. To improve the computational efficiency of the multivariate simplex B-spline method [22], [23], a novel recursive sequential method [24] enabling real-time onboard applications was proposed for modelling the nonlinear aerodynamics of high-performance aircraft. In [25], a novel real-time identification strategy for multivariate splines was proposed to address the aerodynamic uncertainties in the control allocation system, and the computational complexity of the novel multivariate splines was even lower than that of the recursive B-splines method developed in [24].

Time-delayed control (TDC) is a similar control method to INDI whereas the difference among them is that TDC utilizes a diagonal matrix to replace the control effectiveness matrix. The diagonal matrix is selected according to the inequality $\left\| \boldsymbol{I} - \boldsymbol{M}\bar{\boldsymbol{M}}^{-1} \right\| < 1$, proposed in [26] and [27], respectively, where $\boldsymbol{M}$ is the control effectiveness matrix, $\bar{\boldsymbol{M}}$ is the diagonal matrix. As for a controlled system with multi-phase or with time-varying dynamics, the high-performance of the controller with constant diagonal matrix is not always guaranteed during the practice. It is reported that, with constant gains, the TDC controller [28] cannot always guarantee accurate tracking performance for robotic systems with parameter variations. Jin *et al.* [29] have presented auto-tuning method of the diagonal matrix for TDC controller by using an adaptive gain tuning algorithm. However, the actuator dynamics are not taken into consideration and rigorous analysis of stability of the closed-loop system is not given when we take into account the physical constraints of the actuator. In [30], the simulation results have shown that the tracking performance would be degraded terribly when we ignored the actuator dynamics, and sometimes it may even cause instability of the system.

Motivated by the above works, a command filtered model-free robust (CFMFR) attitude controller for an unmanned-aerial vehicle (UAV) is proposed in this paper. As for the first subsystem, INDI is applied to design virtual controller because the elements of the control effectiveness matrix here is the functions with respect to the attitudes of the aircraft, which can be regarded as known. Whereas TDC method is used to design the control law by integrating sliding-mode technique regarding the nominal value of the control effectiveness matrix is unknown. The updating laws of the diagonal matrix are developed by Lyapunov theory. Similar to [17], the actuator biases and the measurement noises, biases, and time delays of the control surface deflection angles are considered in this paper. The improved stable linear filters are also employed to compensate for the filtered errors and the actuator dynamics, ensuring the signals of the filters can remain within a small neighbourhood around the origin, without using the values transmitted from the sensors that measure the control surface deflection angles.

Compared with the existing papers, the contributions of the paper can be concluded as follows: 1) This is a model-free control method. As for the first subsystem, the INDI controller is designed and all the elements of the control effectiveness matrix are functions of the attitude angles of the aircraft, which are regarded as known parameters. Then, for the second subsystem, TDC controller is designed and the diagonal matrix is employed here without any aerodynamic parameters. 2) An adaptive law for the elements of diagonal matrix, is developed to improve the tracking accuracy or attenuate the chattering phenomenon caused by the unreasonable selection of the diagonal matrix. The elements of the diagonal matrix would be adapted according to the tracking errors. This control scheme can make the controller more intelligent. 3) The actuator dynamics are considered in the context of TDC controller, which would cause performance penalty in the real practice. Apart from that, we also take the measurement delays and noises of the actuators into consideration, and improve the compensating scheme.

This paper is organized as follows. In Sec. 2, the model of the aircraft that we wish to control is introduced, and preliminaries are given for some assumptions. In Sec. 3, the command filtered model-free robust attitude controller is proposed, and the updating laws and stability analysis of the closed-loop system are developed by Lyapunov theory. Finally, a numerical simulation is presented in Sec. 4 to demonstrate the efficacy of the proposed control method.

II. PROBLEM FORMULATION AND PRELIMINARIES

A six-degree freedom nonlinear small UAV model is presented as the objective. We consider the following attitude dynamics of the aircraft [31]:

$$\begin{cases} \dot{\boldsymbol{x}}_1 = \boldsymbol{f}_1(\boldsymbol{x}_1) + \Delta\boldsymbol{f}_1(\boldsymbol{x}_1) + \left[\boldsymbol{g}_1(\boldsymbol{x}_1) + \Delta\boldsymbol{g}_1(\boldsymbol{x}_1)\right]\boldsymbol{x}_2 \\ \qquad + \left[\boldsymbol{h}_1(\boldsymbol{x}_1) + \Delta\boldsymbol{h}_1(\boldsymbol{x}_1)\right]\boldsymbol{u} + \boldsymbol{d}_1 \\ \dot{\boldsymbol{x}}_2 = \boldsymbol{f}_2(\boldsymbol{x}_1, \boldsymbol{x}_2) + \Delta\boldsymbol{f}_2(\boldsymbol{x}_1, \boldsymbol{x}_2) \\ \qquad + \left[\boldsymbol{g}_2(\boldsymbol{x}_1, \boldsymbol{x}_2) + \Delta\boldsymbol{g}_2(\boldsymbol{x}_1, \boldsymbol{x}_2)\right]\boldsymbol{u} + \boldsymbol{d}_2 \\ \boldsymbol{y} = \boldsymbol{x}_1 \end{cases} \tag{1}$$

where the state vectors are $\boldsymbol{x}_1 = [\phi\ \alpha\ \beta]^{\mathrm{T}} \in \Re^3$ and $\boldsymbol{x}_2 = [p\ q\ r]^{\mathrm{T}} \in \Re^3$, $\boldsymbol{y}$ is the output of the controlled plant,

$\boldsymbol{u} = [\delta_a\ \delta_e\ \delta_r]^{\mathrm{T}} \in \Re^3$ is the input vector of the vehicle, $\boldsymbol{d}_1$ and $\boldsymbol{d}_2$ are the external disturbances, ϕ, α, β, p, q and r are the roll angle, angle of attack, sideslip angle, roll rate, pitch rate and yaw rate of the aircraft, respectively. The functions $\boldsymbol{f}_i(\bullet)$, $\boldsymbol{g}_i(\bullet)$, and $\boldsymbol{h}_1(\bullet)$ are expressed as follows:

$$\boldsymbol{f}_1(\boldsymbol{x}_1) = \frac{\bar{q}S}{mV_{\mathrm{T}}} \begin{bmatrix} 0 \\ -\left[C_{L,0}+C_{L,\alpha}\alpha+C_{L,\beta}|\beta|+T\sin\alpha\right. \\ \left.-mg\left(\sin\alpha\sin\theta+\cos\alpha\cos\phi\cos\theta\right)\right] \Big/ \cos\beta \\ C_{Y,\beta}\beta - T\sin\beta\cos\alpha + mg\left(\cos\alpha\sin\beta\sin\theta\right. \\ \left.+\cos\beta\sin\phi\cos\theta-\sin\alpha\sin\beta\cos\phi\cos\theta\right) \end{bmatrix}$$

$$\boldsymbol{g}_1(\boldsymbol{x}_1) = \begin{bmatrix} 1 & \sin\phi\tan\theta & \cos\phi\tan\theta \\ -\cos\alpha\tan\beta & 1 & -\sin\alpha\tan\beta \\ \sin\alpha & 0 & -\cos\alpha \end{bmatrix}$$

$$\boldsymbol{h}_1(\boldsymbol{x}_1) = \frac{\bar{q}S}{mV_{\mathrm{T}}\cos\beta} \begin{bmatrix} 0 & 0 & 0 \\ -C_{L,\delta_a} & -C_{L,\delta_e} & -C_{L,\delta_r} \\ C_{Y,\delta_a}\cos\beta & C_{Y,\delta_e}\cos\beta & C_{Y,\delta_r}\cos\beta \end{bmatrix}$$

$$\boldsymbol{f}_2(\boldsymbol{x}_1,\boldsymbol{x}_2) = \begin{bmatrix} c_1pq + c_2qr + \bar{q}Sb\left(c_3C_{l,\beta}\beta + c_4C_{n,\beta}\beta\right) \\ \quad + \frac{\bar{q}Sb^2}{2V_{\mathrm{T}}}\left[c_3\left(C_{l,p}p + C_{l,r}r\right)\right. \\ \quad \left. + c_4\left(C_{n,p}+C_{n,r}r\right)\right] \\ c_5pr - c_6\left(p^2-r^2\right) + \bar{q}S\bar{c}\left(C_{m,0}+C_{m,\alpha}\alpha\right. \\ \quad \left.+C_{m,\beta}\beta\right) + \frac{\bar{q}S\bar{c}^2}{2V_{\mathrm{T}}}c_7C_{m,q} \\ c_8pq - c_1qr + \bar{q}Sb\left(c_4C_{l,\beta}\beta + c_9C_{n,\beta}\beta\right) \\ \quad + \frac{\bar{q}Sb^2}{2V_{\mathrm{T}}}\left[c_4\left(C_{l,p}p + C_{l,r}r\right)\right. \\ \quad \left. + c_9\left(C_{n,p}p + C_{n,r}r\right)\right] \end{bmatrix}$$

$$\boldsymbol{g}_2(\boldsymbol{x}_1,\boldsymbol{x}_2) = \bar{q}S \begin{bmatrix} bc_3C_{l,\delta_a} & bc_3C_{l,\delta_e} & bc_3C_{l,\delta_r} \\ +bc_4C_{n,\delta_a} & +bc_4C_{n,\delta_a} & +bc_4C_{n,\delta_r} \\ \bar{c}c_7C_{m,\delta_a} & \bar{c}c_7C_{m,\delta_e} & \bar{c}c_7C_{m,\delta_r} \\ bc_4C_{l,\delta_a} & bc_4C_{l,\delta_e} & bc_4C_{l,\delta_r} \\ +bc_9C_{n,\delta_a} & +bc_9C_{n,\delta_e} & +bc_9C_{n,\delta_r} \end{bmatrix}$$

The aforementioned aerodynamic coefficients and the parameters related to the introduced vehicle refer to [31].

Herein, a model-free robust controller for the vehicle is proposed. The task of the controller is to stably track the desired command $\boldsymbol{y}_r$ (including ϕ_r, α_r, and β_r) while uncertainties and dynamics of the actuators exist. The ultimate tracking errors are guaranteed to asymptotically converge to a small neighbourhood around the origin. Before the controller is designed, the following reasonable assumptions are made.

Assumption 1 [32]: $\forall c_M \in \Re^+$, every desired command satisfies $\left\|\left[\boldsymbol{y}_r\ \dot{\boldsymbol{y}}_r\right]\right\| \le c_M$, where $\|\bullet\|$ is the 2-norm.

Assumption 2 [32], [33]: The control surface deflection has negligible effect on the aerodynamic force component; i.e., $\boldsymbol{h}_1(\boldsymbol{x}_1)\boldsymbol{u} \approx \boldsymbol{0}$.

According to Assumption 2, the controlled system can be rewritten as follows:

$$\begin{cases} \dot{\boldsymbol{x}}_1 = \boldsymbol{f}_1(\boldsymbol{x}_1) + \boldsymbol{g}_1(\boldsymbol{x}_1)\boldsymbol{x}_2 + \bar{\boldsymbol{d}}_1 \\ \dot{\boldsymbol{x}}_2 = \boldsymbol{f}_2(\boldsymbol{x}_1,\boldsymbol{x}_2) + \boldsymbol{g}_2(\boldsymbol{x}_1,\boldsymbol{x}_2)\boldsymbol{u} + \bar{\boldsymbol{d}}_2 \\ \boldsymbol{y} = \boldsymbol{x}_1 \end{cases} \tag{2}$$

where $\bar{\boldsymbol{d}}_1 = \Delta\boldsymbol{f}_1(\boldsymbol{x}_1) + \Delta\boldsymbol{g}_1(\boldsymbol{x}_1)\boldsymbol{x}_2 + \left[\boldsymbol{h}_1(\boldsymbol{x}_1) + \Delta\boldsymbol{h}_1(\boldsymbol{x}_1)\right]\boldsymbol{u} + \boldsymbol{d}_1$, and $\bar{\boldsymbol{d}}_2 = \Delta\boldsymbol{f}_2(\boldsymbol{x}_1,\boldsymbol{x}_2) + \Delta\boldsymbol{g}_2(\boldsymbol{x}_1,\boldsymbol{x}_2)\boldsymbol{u} + \boldsymbol{d}_2$.

Assumption 3: The composite disturbances $\bar{\boldsymbol{d}}_i\ (i=1,2)$ are bounded. That is, $\forall\varphi_i \in \Re^+$, then, $\bar{\boldsymbol{d}}_i\ (i=1,2)$ satisfy $\left\|\bar{\boldsymbol{d}}_i\right\| \le \varphi_i$.

Remark 1: For the reference signals are passed through the first or second command filter, the reference command should be absolutely smooth. It is reasonable to assume that its first-order derivative is bounded, as stated in Assumption 1. Assumption 2 was introduced in Lee *et al.* [32], which performed a numerical analysis of the influence of the control surfaces on the aerodynamic force and reported that it is negligible. Herein, we consider it as one of the origins of the disturbances. As for Assumption 3, the composite disturbance can be regarded as the difference between the real practice and the nominal values of the controlled plant. Besides, $\boldsymbol{u}$ here is the input of the aircraft, i.e., the control surface deflection. In the practice, the range of the control surface deflection is limited while the $\boldsymbol{u}_d$ (see the section of the controller design and stability analysis) is the designed control law which may exceed the bound of the control $\boldsymbol{u}$. The physical limits would restrict the control $\boldsymbol{u}$ keep staying in the bound no matter how the designed control law $\boldsymbol{u}_d$ changes. So it is reasonable to assume the disturbances $\bar{\boldsymbol{d}}_1$ and $\bar{\boldsymbol{d}}_2$ are all bounded. The positive constants φ_i mentioned in Assumption 3, whose exact range cannot be determined, are simply utilized to analyze the stability of the closed-loop system.

III. CONTROLLER DESIGN AND STABILITY ANALYSIS

In this section, the CFMFR controller is developed, and the updating laws of the elements of the diagonal matrix are constructed by using Lyapunov theory. The stability of the resulting closed-loop system is analyzed at the end of the section.

The controller design process comprises the following two steps.

Step 1: Consider the first subsystem:

$$\dot{\boldsymbol{x}}_1 = \boldsymbol{f}_1(\boldsymbol{x}_1) + \boldsymbol{g}_1(\boldsymbol{x}_1)\boldsymbol{x}_2 + \bar{\boldsymbol{d}}_1 \tag{3}$$

Regarding the composite disturbance as a part of the function $\boldsymbol{f}_1(\boldsymbol{x}_1)$ and taking the first-order Taylor series

expansion around the solution $[\boldsymbol{x}_{1,0}, \boldsymbol{x}_{2,0}]$ results in

$$\begin{aligned}\dot{\boldsymbol{x}}_1 \cong \dot{\boldsymbol{x}}_{1,0} + \frac{\partial}{\partial \boldsymbol{x}_1}\left[\boldsymbol{f}_1(\boldsymbol{x}_1) + \bar{\boldsymbol{d}}_1 \right. \\ \left. + \boldsymbol{g}_1(\boldsymbol{x}_1)\boldsymbol{x}_2\right]\Big|_{\substack{\boldsymbol{x}_1=\boldsymbol{x}_{1,0} \\ \boldsymbol{x}_2=\boldsymbol{x}_{2,0}}} (\boldsymbol{x}_1 - \boldsymbol{x}_{1,0}) \\ + \frac{\partial}{\partial \boldsymbol{x}_2}\left[\boldsymbol{f}_1(\boldsymbol{x}_1) + \bar{\boldsymbol{d}}_1 + \boldsymbol{g}_1(\boldsymbol{x}_1)\boldsymbol{x}_2\right]\Big|_{\substack{\boldsymbol{x}_1=\boldsymbol{x}_{1,0} \\ \boldsymbol{x}_2=\boldsymbol{x}_{2,0}}} (\boldsymbol{x}_2 - \boldsymbol{x}_{2,0}) + \phi_1\end{aligned} \tag{4}$$

where ∂ denotes a partial differential operator, and ϕ_1 is the linearization error, which arises from the expansion process and can be small when the sampling rate is sufficiently high. Equation (4) can be rewritten as follows:

$$\dot{\boldsymbol{x}}_1 = \dot{\boldsymbol{x}}_{1,0} + \boldsymbol{A}_1 \Delta \boldsymbol{x}_1 + \boldsymbol{g}_1(\boldsymbol{x}_{1,0})\Delta \boldsymbol{x}_2 + \phi_1 \tag{5}$$

where $\Delta \boldsymbol{x}_1 = \boldsymbol{x}_1 - \boldsymbol{x}_{1,0}$, $\Delta \boldsymbol{x}_2 = \boldsymbol{x}_2 - \boldsymbol{x}_{2,0}$, $\boldsymbol{A}_1 = \frac{\partial}{\partial \boldsymbol{x}_1}\left[\boldsymbol{f}_1(\boldsymbol{x}_1) + \boldsymbol{g}_1(\boldsymbol{x}_1)\boldsymbol{x}_2\right]\Big|_{\substack{\boldsymbol{x}_1=\boldsymbol{x}_{1,0} \\ \boldsymbol{x}_2=\boldsymbol{x}_{2,0}}}$. According to the assumptions introduced in the previous section, compared with the incremental quality $\Delta \boldsymbol{x}_2$, $\Delta \boldsymbol{x}_1$ can be neglected for the system because of the time-scale separation (TSS) principle [34], [35]. As a result, we can rewrite (5) as

$$\dot{\boldsymbol{x}}_1 = \dot{\boldsymbol{x}}_{1,0} + \boldsymbol{g}_1(\boldsymbol{x}_{1,0})\Delta \boldsymbol{x}_2 + \bar{\boldsymbol{\phi}}_1 \tag{6}$$

where $\bar{\phi}_1 = \boldsymbol{A}_1 \Delta \boldsymbol{x}_1 + \phi_1$ is the composed linearization error.

According to incremental nonlinear dynamic inversion, we can design the incremental virtual control law for the first subsystem of the controlled plant:

$$\Delta \boldsymbol{x}_{2d} = -\left[\boldsymbol{g}_1(\boldsymbol{x}_{1,0})\right]^{-1}\left(k_1 \tilde{\boldsymbol{x}}_1 + \dot{\boldsymbol{x}}_{1,0} - \dot{\boldsymbol{y}}_c\right) \tag{7}$$

where $k_1 > 0$ is the controller design parameter, $\boldsymbol{y}_c$ is the smooth signal that can be obtained by passing the reference signal $\boldsymbol{y}_r$ through the filter, and $\tilde{\boldsymbol{x}}_1 = \boldsymbol{x}_1 - \boldsymbol{y}_c$ is the tracking error. The virtual control law is designed by adding the introduced incremental intermediate $\Delta \boldsymbol{x}_{2d}$ to the state quantities $\boldsymbol{x}_{2,0}$. Therefore, $\boldsymbol{x}_{2d} = \boldsymbol{x}_{2,0} + \Delta \boldsymbol{x}_{2d}$. The second order low pass command filter introduced in [7] is applied to obtain the smooth intermediate control law.

Remark 2: According to Lemma 1 in [32], the function $\boldsymbol{g}_1(\boldsymbol{x}_1)$ is invertible for that the set of rows of $\boldsymbol{g}_1(\boldsymbol{x}_1)$ is linearly independent. Therefore, the incremental intermediate control law can be implemented without any assumptions and specific conditions.

The compensated signal ξ_1, which should be designed to compensate for the errors resulting from the introduced command filter, can be obtained from the following stable filter:

$$\dot{\boldsymbol{\xi}}_1 = -k_1 \xi_1 + \boldsymbol{g}_1(\boldsymbol{x}_{1,0})(\boldsymbol{x}_{2c} - \boldsymbol{x}_{2d}) + \boldsymbol{g}_1(\boldsymbol{x}_{1,0})\xi_2 \tag{8}$$

where $\boldsymbol{x}_{2c}$ is the smooth signal obtained by passing $\boldsymbol{x}_{2d}$ through the command filter. ξ_2 is also a compensated signal and will be given in the next step.

Let $\tilde{\boldsymbol{x}}_2 = \boldsymbol{x}_2 - \boldsymbol{x}_{2c}$ be the tracking error. The dynamics of the tracking error $\tilde{\boldsymbol{x}}_1$ can be analyzed as follows:

$$\begin{aligned}\dot{\tilde{\boldsymbol{x}}}_1 &= \dot{\boldsymbol{x}}_1 - \dot{\boldsymbol{y}}_c \\ &= \dot{\boldsymbol{x}}_{1,0} + \boldsymbol{g}_1(\boldsymbol{x}_{1,0})\Delta \boldsymbol{x}_2 + \bar{\phi}_1 - \dot{\boldsymbol{y}}_c \\ &= \dot{\boldsymbol{x}}_{1,0} + \boldsymbol{g}_1(\boldsymbol{x}_{1,0})[\boldsymbol{x}_{2d} + (\boldsymbol{x}_{2c} - \boldsymbol{x}_{2d}) \\ &\quad + (\boldsymbol{x}_2 - \boldsymbol{x}_{2c}) - \boldsymbol{x}_{2,0}] + \bar{\phi}_1 - \dot{\boldsymbol{y}}_c \\ &= \dot{\boldsymbol{x}}_{1,0} + \boldsymbol{g}_1(\boldsymbol{x}_{1,0})\Delta \boldsymbol{x}_{2d} + \boldsymbol{g}_1(\boldsymbol{x}_{1,0})(\boldsymbol{x}_{2c} - \boldsymbol{x}_{2d}) \\ &\quad + \boldsymbol{g}_1(\boldsymbol{x}_{1,0})\tilde{\boldsymbol{x}}_2 + \bar{\phi}_1 - \dot{\boldsymbol{y}}_c\end{aligned} \tag{9}$$

Substituting the virtual control law (7) into (9), we have

$$\dot{\tilde{\boldsymbol{x}}}_1 = -k_1 \tilde{\boldsymbol{x}}_1 + \boldsymbol{g}_1(\boldsymbol{x}_{1,0})(\boldsymbol{x}_{2c} - \boldsymbol{x}_{2d}) + \boldsymbol{g}_1(\boldsymbol{x}_{1,0})\tilde{\boldsymbol{x}}_2 + \bar{\phi}_1 \tag{10}$$

Let $z_1 = \tilde{\boldsymbol{x}}_1 - \xi_1$ be the compensated error and whose dynamics can be expressed as follows:

$$\dot{\boldsymbol{z}}_1 = \dot{\tilde{\boldsymbol{x}}}_1 - \dot{\boldsymbol{\xi}}_1 = -c_1 \boldsymbol{z}_1 + \boldsymbol{g}_1(\boldsymbol{x}_{1,0})\boldsymbol{z}_2 + \bar{\phi}_1 \tag{11}$$

Consider the following Lyapunov function $V_1 : \boldsymbol{D}_{z_1} \to \Re$

$$V_1 = \frac{1}{2}\boldsymbol{z}_1^{\mathrm{T}}\boldsymbol{z}_1 \tag{12}$$

where $\boldsymbol{D}_{z_1} \subset \Re^3$ is the domain of the function and contains the origin. In accordance with (11), the time derivative of V_1 is given as

$$\begin{aligned}\dot{V}_1 &= \boldsymbol{z}_1^{\mathrm{T}}\dot{\boldsymbol{z}}_1 \\ &= \boldsymbol{z}_1^{\mathrm{T}}\left[-c_1 \boldsymbol{z}_1 + \boldsymbol{g}_1(\boldsymbol{x}_{1,0})\boldsymbol{z}_2 + \bar{\phi}_1\right] \\ &= -c_1 \boldsymbol{z}_1^{\mathrm{T}}\boldsymbol{z}_1 + \boldsymbol{z}_1^{\mathrm{T}}\boldsymbol{g}_1(\boldsymbol{x}_{1,0})\boldsymbol{z}_2 + \boldsymbol{z}_1^{\mathrm{T}}\bar{\phi}_1\end{aligned} \tag{13}$$

where $\boldsymbol{z}_2 = \tilde{\boldsymbol{x}}_2 - \xi_2$ is the compensated error for the second subsystem, ξ_2 the compensated item given in the second step.

According to (13), $\boldsymbol{z}_1$ is asymptotically stable under the effect of the virtual control law (7) if the tracking error $\boldsymbol{z}_2$ converges to zero.

Step 2: The control law is designed in this step. The dynamics of the actuators are considered, and the corresponding compensated schemes are complemented. Consider the second subsystem:

$$\dot{\boldsymbol{x}}_2 = \boldsymbol{f}_2(\boldsymbol{x}) + \boldsymbol{g}_2(\boldsymbol{x})\boldsymbol{u} \tag{14}$$

where $\boldsymbol{x} = \left[\boldsymbol{x}_1^{\mathrm{T}}, \boldsymbol{x}_2^{\mathrm{T}}\right]^{\mathrm{T}}$. Taking the first-order Taylor series expansion around the solution $[\boldsymbol{x}_0, \boldsymbol{u}_0]$ yields

$$\begin{aligned}\dot{\boldsymbol{x}}_2 \cong \dot{\boldsymbol{x}}_{2,0} + \frac{\partial}{\partial \boldsymbol{x}}\left[\boldsymbol{f}_2(\boldsymbol{x}) + \boldsymbol{g}_2(\boldsymbol{x})\boldsymbol{u}\right]\Big|_{\substack{\boldsymbol{x}=\boldsymbol{x}_0 \\ \boldsymbol{u}=\boldsymbol{u}_0}} (\boldsymbol{x} - \boldsymbol{x}_0) \\ + \frac{\partial}{\partial \boldsymbol{u}}\left[\boldsymbol{f}_2(\boldsymbol{x}) + \boldsymbol{g}_2(\boldsymbol{x})\boldsymbol{u}\right]\Big|_{\substack{\boldsymbol{x}=\boldsymbol{x}_0 \\ \boldsymbol{u}=\boldsymbol{u}_0}} (\boldsymbol{u} - \boldsymbol{u}_0)\end{aligned} \tag{15}$$

Similarly, let ϕ_2 be the error arising from the linearization process. Hence, we can rewrite (15) as

$$\dot{\boldsymbol{x}}_2 = \dot{\boldsymbol{x}}_{2,0} + \boldsymbol{A}_2 \Delta \boldsymbol{x} + \boldsymbol{g}_2(\boldsymbol{x}_0)\,\Delta \boldsymbol{u} + \phi_2 \tag{16}$$

where $\Delta \boldsymbol{x} = \boldsymbol{x} - \boldsymbol{x}_0$, $\Delta \boldsymbol{u} = \boldsymbol{u} - \boldsymbol{u}_0$, and $\boldsymbol{A}_2 = \frac{\partial}{\partial \boldsymbol{x}}\left[\boldsymbol{f}_2(\boldsymbol{x}) + \boldsymbol{g}_2(\boldsymbol{x})\,\boldsymbol{u}\right]\Big|_{\substack{\boldsymbol{x}=\boldsymbol{x}_0 \\ \boldsymbol{u}=\boldsymbol{u}_0}}$. According to the TSS principle, compared with the incremental quality $\Delta \boldsymbol{u}$, $\Delta \boldsymbol{x}$ can be neglected. As a result, we can rewrite (16) as

$$\dot{\boldsymbol{x}}_2 = \dot{\boldsymbol{x}}_{2,0} + \boldsymbol{A}_2 \Delta \boldsymbol{x} + \boldsymbol{g}_2(\boldsymbol{x}_0)\,\Delta \boldsymbol{u} + \phi_2 \tag{17}$$

where $\bar{\phi}_2 = \boldsymbol{A}_2 \Delta \boldsymbol{x} + \phi_2$ is the composed error.

According to TDC controller design, let $\boldsymbol{u}$ be the controller, we can conclude that

$$\boldsymbol{u} = \bar{\boldsymbol{G}}_{inv} \dot{\boldsymbol{x}}_2 + \boldsymbol{h} \tag{18}$$

where $\bar{\boldsymbol{G}}_{inv}$ is the diagonal matrix, $\boldsymbol{h} = \left[\boldsymbol{g}_2^{-1}(\boldsymbol{x}_1, \boldsymbol{x}_2) - \bar{\boldsymbol{G}}_{inv}\right] \dot{\boldsymbol{x}}_2 - \boldsymbol{g}_2^{-1}(\boldsymbol{x}_1, \boldsymbol{x}_2) \boldsymbol{f}_2(\boldsymbol{x}_1, \boldsymbol{x}_2)$.

Then the controller $\boldsymbol{u}_d$ can de designed as follows:

$$\boldsymbol{u}_d = \bar{\boldsymbol{G}}_{inv}\left(\dot{\boldsymbol{x}}_{2c} - 2\lambda \boldsymbol{z}_2 - k_2 \xi_2 - \lambda^2 \int \boldsymbol{z}_2 dt\right) + \boldsymbol{h}_{(t-L)} + (\mathrm{Fil}(\boldsymbol{u}_{d0}) - \boldsymbol{u}_{c0}) \tag{19}$$

where $\lambda \in \boldsymbol{R}^+$ and $k_2 \in \boldsymbol{R}^+$ are the design parameter, $\boldsymbol{h}_{(t-L)}$ the value of $\boldsymbol{h}$ at time $(t-L)$, L the sampling time. Let $t_0 = t - L$, then $\boldsymbol{h}_{(t-L)} = \boldsymbol{u}_{c0} - \bar{\boldsymbol{G}}^{-1} \dot{\boldsymbol{x}}_{2,0}$, where $\boldsymbol{u}_{c0}$ and $\dot{\boldsymbol{x}}_{2,0}$ are the value of $\boldsymbol{u}$ and $\dot{\boldsymbol{x}}_2$ at time t_0, respectively. The function Fil $(*)$ is a low-pass filter which is used to approximate the actuator dynamics.

Let ξ_2 be the output signal of the first-order low-pass filter (LPF), which is designed as follows:

$$\dot{\boldsymbol{\xi}}_2 = -k_2 \xi_2 + \bar{\boldsymbol{G}}_{inv}(\mathrm{Fil}(\boldsymbol{u}_d) - \boldsymbol{u}_d) \tag{20}$$

Then, the controller $\boldsymbol{u}$ is transformed as follows:

$$\boldsymbol{u} = \bar{\boldsymbol{G}}_{inv} \dot{\boldsymbol{x}}_2 + \boldsymbol{h} = \bar{\boldsymbol{G}}_{inv}\left(\dot{\boldsymbol{x}}_2 - \dot{\boldsymbol{\xi}}_2\right) + \bar{\boldsymbol{G}}_{inv} \dot{\boldsymbol{\xi}}_2 + \boldsymbol{h} \tag{21}$$

The controller $\boldsymbol{u}$ can also be expressed as follows:

$$\boldsymbol{u} = \boldsymbol{u}_d + (\mathrm{Fil}(\boldsymbol{u}_d) - \boldsymbol{u}_d) + (\boldsymbol{u}_c - \mathrm{Fil}(\boldsymbol{u}_d)) \tag{22}$$

Substituting (20) and (22) into (21) results in

$$\boldsymbol{u}_d = \bar{\boldsymbol{G}}_{inv}\left(\dot{\boldsymbol{x}}_2 - \dot{\boldsymbol{\xi}}_2\right) - k_2 \bar{\boldsymbol{G}}_{inv} \xi_2 + (\mathrm{Fil}(\boldsymbol{u}_d) - \boldsymbol{u}_c) + \boldsymbol{h} \tag{23}$$

Combining (19) and (23), we can obtain the following equations:

$$\begin{aligned} &\bar{\boldsymbol{G}}_{inv}\left(\dot{\boldsymbol{x}}_2 - \dot{\boldsymbol{\xi}}_2\right) - k_2 \bar{\boldsymbol{G}}_{inv} \xi_2 + (\mathrm{Fil}(\boldsymbol{u}_d) - \boldsymbol{u}_c) + \boldsymbol{h} \\ &\quad = \bar{\boldsymbol{G}}_{inv}\left(\dot{\boldsymbol{x}}_{2c} - 2\lambda \boldsymbol{z}_2 - k_2 \xi_2 - \lambda^2 \int \boldsymbol{z}_2 dt\right) + \boldsymbol{h}_{(t-L)} \\ &\qquad + (\mathrm{Fil}(\boldsymbol{u}_{d0}) - \boldsymbol{u}_{c0}) \end{aligned} \tag{24}$$

$$\bar{\boldsymbol{G}}_{inv}\left(\dot{\boldsymbol{z}}_2 + 2\lambda \boldsymbol{z}_2 + \lambda^2 \int \boldsymbol{z}_2 dt\right) = (\boldsymbol{\varepsilon}_1 + \boldsymbol{\varepsilon}_2 - \boldsymbol{\varepsilon}_3) \tag{25}$$

where $\boldsymbol{\varepsilon}_1 = \left(\boldsymbol{h}_{(t-L)} - \boldsymbol{h}\right)$, $\boldsymbol{\varepsilon}_2 = (\boldsymbol{u}_c - \boldsymbol{u}_{c0})$, and $\boldsymbol{\varepsilon}_3 = (\mathrm{Fil}(\boldsymbol{u}_d) - \mathrm{Fil}(\boldsymbol{u}_{d0}))$. A sliding surface is then designed as follows:

$$\boldsymbol{s} = \boldsymbol{z}_2 + \lambda \int \boldsymbol{z}_2 dt \tag{26}$$

Substituting (26) into (25) results in

$$(\dot{\boldsymbol{s}}_2 + \lambda \boldsymbol{s}_2) = \bar{\boldsymbol{G}}(\boldsymbol{\varepsilon}_1 + \boldsymbol{\varepsilon}_2 - \boldsymbol{\varepsilon}_3) \tag{27}$$

where $\bar{\boldsymbol{G}} = \left(\bar{\boldsymbol{G}}_{inv}\right)^{-1}$.

The well-known stability condition TDC is established by Youcef-Toumi and Hsia independently in [26], [27], given as follows according to the real second subsystem of the controlled plant.

$$\left\| \boldsymbol{I} - \boldsymbol{g}_2(\boldsymbol{x}_1, \boldsymbol{x}_2)\, \bar{\boldsymbol{G}}_{inv} \right\| < 1 \tag{28}$$

When the closed-loop system is stable with the stability criterion (28), $\boldsymbol{\varepsilon}_1 = \left(\boldsymbol{h}_{(t-L)} - \boldsymbol{h}\right)$ is bounded because $\boldsymbol{h}$ is the sum of continuous terms and bounded discontinuous terms, and $(\boldsymbol{\varepsilon}_2 - \boldsymbol{\varepsilon}_3)$ is also bounded for that magnitude and rate of the actuator and the introduced LPF are all saturated.

According to (23), the incremental control law can be obtained as follows:

$$\Delta \boldsymbol{u}_d = \bar{\boldsymbol{G}}_{inv}\left(\dot{\boldsymbol{x}}_{2c} - 2\lambda \boldsymbol{z}_2 - k_2 \xi_2 - \lambda^2 \int \boldsymbol{z}_2 dt - \dot{\boldsymbol{x}}_{20}\right) \tag{29}$$

From (27), it is obvious that $\|\boldsymbol{s}\|$ would be very small when $\left\|\bar{\boldsymbol{G}}_{inv}\right\|$ increased. However, some research work also indicates that too large value of $\left\|\bar{\boldsymbol{G}}_{inv}\right\|$ arises chattering of actuator dynamics, and this chattering may cause mechanical and electronic damage to the aircraft. So, selection of the parameter of the diagonal matrix $\bar{\boldsymbol{G}}_{inv}$ is a hard nut. We also found that the desired gain $\bar{\boldsymbol{G}}_{inv}$ at one point of the flight channel may not be the best option for another one. Therefore, the further research on practical adaptive tuning algorithm of the gain $\bar{\boldsymbol{G}}_{inv}$ is demanded.

The updating laws of the gain $\bar{\boldsymbol{G}}_{inv}$ are proposed as follows:

$$\begin{cases} \bar{G}_{inv,i} = \dfrac{\lambda}{a_i}, & if\ \dfrac{\lambda}{a_i} \le \bar{G}_{inv,i} \\ \dot{\bar{G}}_{inv,i} = a_i\left[|s_i|^{\gamma} - \omega_i \left|\bar{G}_{inv,i}\right|^{\chi} sgn\left(\bar{G}_{inv,i}\right)\right], & \\ \qquad\qquad if\ \sigma_i < \bar{G}_{inv,i} < \dfrac{\lambda}{a_i} & \\ \bar{G}_{inv,i} = \sigma_i \qquad if\ \bar{G}_{inv,i} \le \sigma_i & \end{cases} \tag{30}$$

where $\bar{G}_{inv,i}$ is the i-th element of the diagonal matrix, $\dot{\bar{G}}_{inv,i}$ is the time derivative of the parameter $\bar{G}_{inv,i}$, s_i is the i-th element of the sliding variable $\boldsymbol{s} = [s_1 s_2 s_3]^{\mathrm{T}}$, $a_i > 0$ is the adaptation law, ω_i is the leakage factor of i-th element to prevent parameter drift resulting in chattering of actuator dynamics according to above discussion, $\sigma_i > 0$ is a small positive constant which sets a threshold for each parameter, $\gamma > 1$, $\chi > 0$, $sgn(*)$ is the sign function.

Consider the following Lyapunov function V_2 [29] : $\boldsymbol{D}_{z_2} \times \boldsymbol{D}_{\bar{G}_{inv}} \to \Re$:

$$V_2 = \sum_{i=1}^{3}\left[\frac{1}{\gamma}|s_i|^{\gamma} + \frac{1}{2}\left(\bar{G}_{inv,i}\right)^2\right] \tag{31}$$

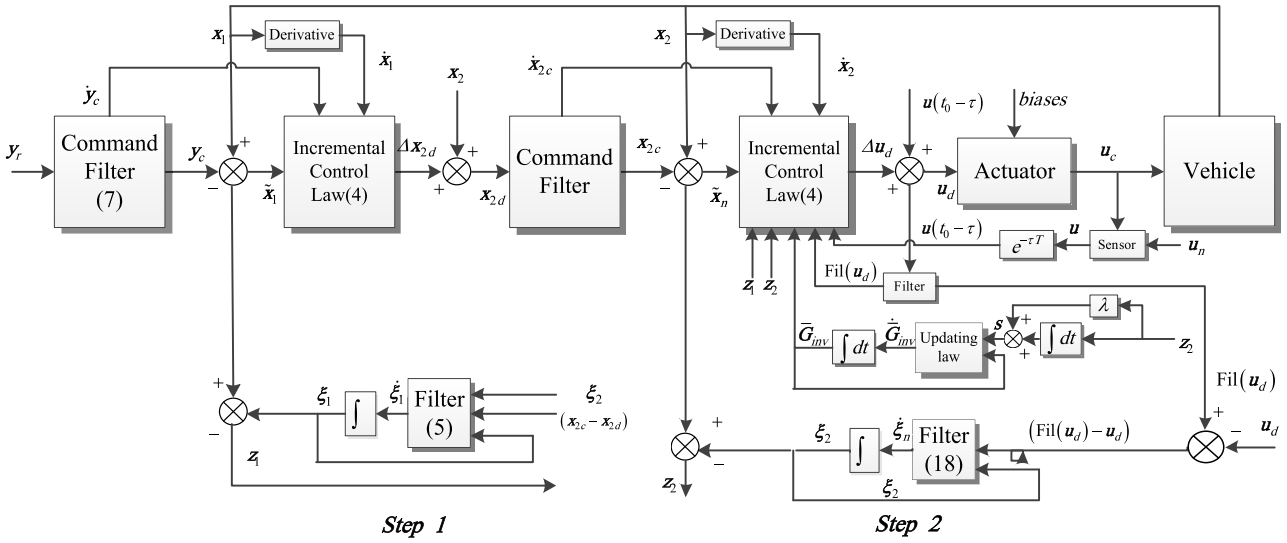

FIGURE 1. Block diagram of the control structure (the number insider is the equation number).

where $\boldsymbol{D}_{z_2} \subset \Re^3$ and $\boldsymbol{D}_{\bar{G}_{inv}} \subset \Re^3$ is the domain of the function and contains the origin. In accordance with (27) and (30), the time derivative of V_2 is given as

$$\begin{aligned}\dot{V}_2 &= \sum_{i=1}^{3}\left\{\left[-\lambda s_i + \overline{G}_i\left(\varepsilon_{1,i}+\varepsilon_{2,i}-\varepsilon_{3,i}\right)\right]|s_i|^{\gamma-1}\,\mathrm{sgn}\left(s_i\right)\right. \\ &\quad \left.+a_i\overline{G}_{inv,i}\left(\left[|s_i|^{\gamma}-\omega_i\left|\overline{G}_{inv,i}\right|^{\chi}\mathrm{sgn}\left(\overline{G}_{inv,i}\right)\right]\right)\right\} \\ &= \sum_{i=1}^{3}\left[\left(-\lambda+a_i\overline{G}_{inv,i}\right)|s_i|^{\gamma}\right. \\ &\quad \left.+\overline{G}_i\left(\varepsilon_{1,i}+\varepsilon_{2,i}-\varepsilon_{3,i}\right)|s_i|^{\gamma-1}\,\mathrm{sgn}\left(s_i\right)\right] \\ &\quad -\sum_{i=1}^{3}a_i\omega_i\left|\overline{G}_{inv,i}\right|^{x+1} \end{aligned} \tag{32}$$

It is obvious that $-\sum_{i=1}^{3}a_i\omega_i\left|\bar{G}_{inv,i}\right|^{\chi+1} < 0$. Hence, (32) becomes

$$\dot{V}_2 < \sum_{i=1}^{3}\left[\left(-\lambda+a_i\bar{G}_{inv,i}\right)|s_i|^{\gamma}+\bar{G}_{inv,i}\varepsilon_{\max,i}\,|s_i|^{\gamma-1}\right] \tag{33}$$

where $\varepsilon_{\max,i} = \left|\left(\varepsilon_{1,i}+\varepsilon_{2,i}-\varepsilon_{3,i}\right)sgn\left(s_i\right)\right|$. Let $c_{2,i} = \left(\lambda - a_i\bar{G}_{inv,i}\right)$, $\kappa_i = \bar{G}_{inv,i}\varepsilon_{\max,i}$, then

$$\dot{V}_2 < \sum_{i=1}^{3}-\left(c_{2,i}\,|s_i|-\kappa_i\right)|s_i|^{\gamma-1} \tag{34}$$

From (34), it is concluded that $\dot{V}_2 \le 0$ when $|s_i| \ge \kappa_i/c_{2,i}$. It also implies that all the signals including $\bar{G}_{inv,i}$ are bounded. According to the definition of the sliding surface $\boldsymbol{s} = \boldsymbol{z}_2 + \lambda\int \boldsymbol{z}_2 dt$, the compensated tracking error $\boldsymbol{z}_2$ is bounded. The stability of the tracking errors are not analyzed for that the aforementioned stability-analysis procedures mainly focus on compensated tracking errors. According to the definition of the compensated tracking errors, the stability analysis of the compensated signals must be accomplished.

Remark 3: The updating law of the gain (30) can reduce the chattering performance [36] of the sliding mode variable (26) for that the gain would increase when the sliding mode variable increased while it would decrease as the sliding mode variable reduces.

A Lyapunov function $V_\xi : \boldsymbol{D}_{\xi_1} \times \boldsymbol{D}_{\xi_2} \to \Re$ is chosen as follows:

$$\dot{V}_\xi = \frac{1}{2}\xi_1^{\mathrm{T}}\xi_1 + \frac{1}{2}\xi_2^{\mathrm{T}}\xi_2 \tag{35}$$

where $\boldsymbol{D}_{\xi_1} \subset \Re^3$ and $\boldsymbol{D}_{\xi_2} \subset \Re^3$ are the domains of the function and contains the origin. In accordance with (8) and (20), the time derivative of V_ξ is written as

$$\begin{aligned}\dot{V}_\xi &= \xi_1^{\mathrm{T}}\dot{\xi}_1 + \xi_2^{\mathrm{T}}\dot{\xi}_2 \\ &= \xi_1^{\mathrm{T}}\left[-c_1\xi_1 + \boldsymbol{g}_1\left(\boldsymbol{x}_{1,0}\right)\left(\boldsymbol{x}_{2c}-\boldsymbol{x}_{2d}\right)+\boldsymbol{g}_1\left(\boldsymbol{x}_{1,0}\right)\xi_2\right] \\ &\quad +\xi_2^{\mathrm{T}}\left[-k\xi_2+\bar{\boldsymbol{G}}_{inv}\left(\mathrm{Fil}(\boldsymbol{u}_d)-\boldsymbol{u}_d\right)\right] \\ &= -c_1\xi_1^{\mathrm{T}}\xi_1 - k\xi_2^{\mathrm{T}}\xi_2 + \xi_1^{\mathrm{T}}\boldsymbol{g}_1\left(\boldsymbol{x}_{1,0}\right)\left(\boldsymbol{x}_{2c}-\boldsymbol{x}_{2d}\right) \\ &\quad +\xi_1^{\mathrm{T}}\boldsymbol{g}_1\left(\boldsymbol{x}_{1,0}\right)\xi_2 + \xi_2^{\mathrm{T}}\bar{\boldsymbol{G}}_{inv}\left(\mathrm{Fil}(\boldsymbol{u}_d)-\boldsymbol{u}_d\right) \end{aligned} \tag{36}$$

Some assumptions are introduced here:

Assumption 4: $\forall\rho_1 \in \Re^+$ and $\forall\rho_2 \in \Re^+$, $\rho_i\,(i=1,2)$ satisfy $\|\boldsymbol{x}_{2c}-\boldsymbol{x}_{2d}\| \le \rho_1$ and $\|\boldsymbol{u}-\boldsymbol{u}_d\| \le \rho_2$.

Assumption 5: There is a positive constant $g_{1,\max}$ such that $\left\|\boldsymbol{g}_1(\bullet)\right\| \le g_{1,\max}$.

Assumption 6: $\forall\rho_3 \in \Re^+$, ρ_3 satisfies $\left\|\mathrm{Fil}\left(\boldsymbol{u}_d\right)-\boldsymbol{u}_d\right\| \le \rho_3$.

Remark 4: Most actuators have the low-pass property [37], [38]. The introduced second-order filter with the magnitude, rate, and bandwidth limitations is an LPF by nature. The function $\boldsymbol{g}_1(\bullet)$ is bounded on the specific set because of the continuity. So, Assumption 4 and 5 are

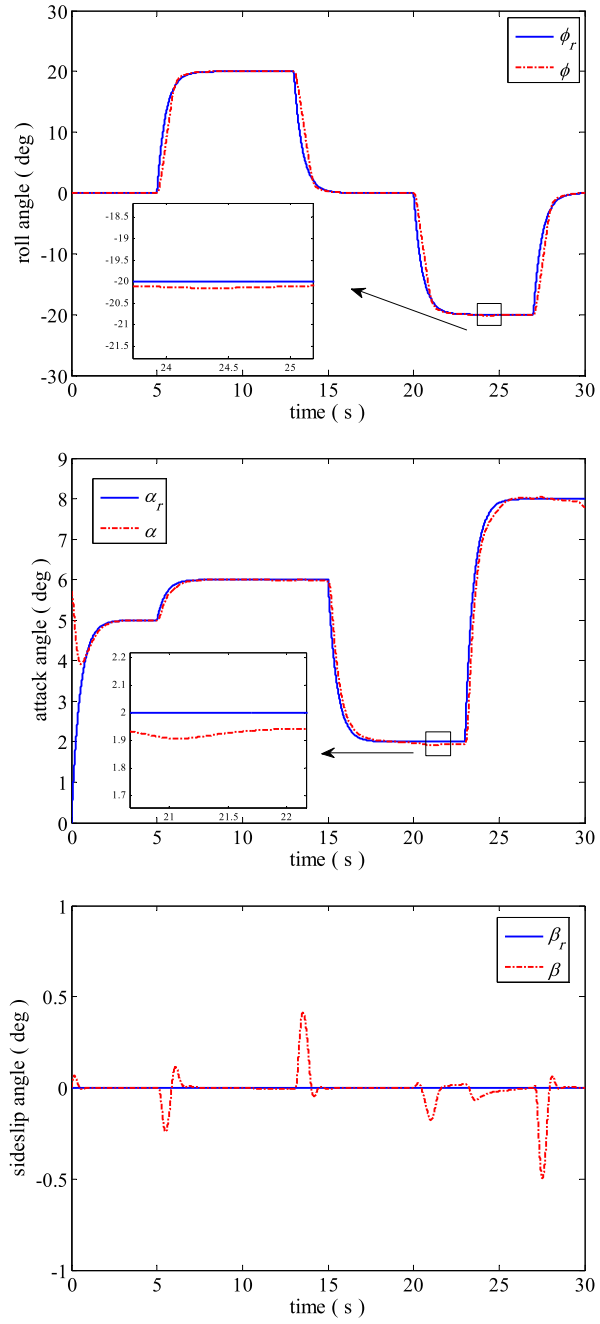

FIGURE 2. Curves of the attitude angles with the constant value $\bar{G}_{inv,i} = diag(0.05, 0.05, 0.05)$.

reasonable. According to property of the LPF, $\forall T \in [t_0, \infty)$, then $t > T$, $\|\mathrm{Fil}(\boldsymbol{u}_d) - \boldsymbol{u}_d\| \to 0$. Thus, ρ_3 can be very small when the closed-loop system remains stable.

According to Young's inequality and principles of the norm of the matrices, the following inequalities are obtained:

$$\left\|\xi_1^{\mathrm{T}}\boldsymbol{g}_1\left(x_{1,0}\right)\xi_2\right\| \leq \sigma_1\|\xi_1\|\|\xi_2\| \leq \frac{g_{1,\max}}{2}\left(\|\xi_1\|^2+\|\xi_2\|^2\right) \tag{37}$$

$$\left\|\xi_1^{\mathrm{T}}\boldsymbol{g}_1\left(\boldsymbol{x}_{1,0}\right)\left(\boldsymbol{x}_{2c}-\boldsymbol{x}_{2d}\right)\right\| \leq g_{1,\max}\rho_1\|\xi_1\| \tag{38}$$

$$\left\|\xi_2^{\mathrm{T}}\bar{\boldsymbol{G}}_{inv}\left(\mathrm{Fil}(\boldsymbol{u}_d)-\boldsymbol{u}_d\right)\right\| \leq \frac{\lambda\rho_3}{a_i}\|\xi_2\| \tag{39}$$

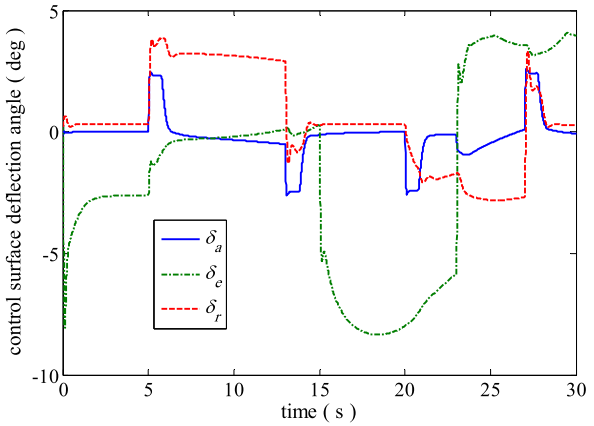

FIGURE 3. Curves of the control surface deflection angles with the constant value $\bar{G}_{inv,i} = diag(0.05, 0.05, 0.05)$.

Substituting (37), (38), and (39) into (36), we can get

$$\dot{V}_\xi \leq -\left(c_1-\frac{g_{1,\max}}{2}\right)\|\xi_1\|^2-\left(k-\frac{g_{1,\max}}{2}\right)\|\xi_2\|^2 +g_{1,\max}\rho_1\|\xi_1\|+\frac{\lambda\rho_3}{a_i}\|\xi_2\| \leq -4k_0V_\xi+\psi\rho\sqrt{V_\xi} \tag{40}$$

where $k_0 = 0.5\min\left\{\left(c_1-\frac{g_{1,\max}}{2}\right),\left(k-\frac{g_{1,\max}}{2}\right)\right\}$, $\psi\rho = \max\left\{g_{1,\max}\rho_1, \frac{\lambda\rho_3}{a_i}\right\}$. It should be noted that selection of the design parameters c_1, k must satisfy the conditions that $c_1 > \frac{g_{1,\max}}{2}$, $k > \frac{g_{1,\max}}{2}$, $\boldsymbol{g}_1$ is a function with respect to the attitude angles, of which the scope is easy to determine.

Hence, the compensated signals ξ_i satisfy this following bound:

$$\|\xi_i\| \leq \frac{\psi\rho}{2k_0}\left(1-e^{-2k_0t}\right) \tag{41}$$

It indicates that the compensated signals are bounded [36]. In [17], stability analysis of the traditional command filter [6], [7] is introduced when actuator biases or actuator measurement errors occur. It shows that there is an increase in the ultimate errors of the compensated signals if biases and measurement errors exist. The above improved stable linear filters can make the compensated signals converge to small neighborhood around the origin even when actuator biases and measurement errors occur simultaneously for that the LPF filters are introduced in the stable linear filters. So, the compensated errors and compensated signals are all bounded based on above discussion. According to the definition of the compensated errors $z_i = \tilde{\boldsymbol{x}}_i - \xi_i$ $(i = 1, 2)$, it implies that the tracking errors $\tilde{\boldsymbol{x}}_i$ $(i = 1, 2)$ and other control signals are bounded over any time interval.

The foregoing analysis yields the following theorem.

Theorem 1: For the nonlinear system defined in (1), under Assumptions 1-6, with the incremental control laws of (7) and (29), the stable linear filters designed by (8) and (20) to compensate for the actuator dynamics and the filter errors caused by the second-order command filter, and the updating law of the elements of the diagonal matrix, we can obtain that all of the signals of the closed-loop system are bounded

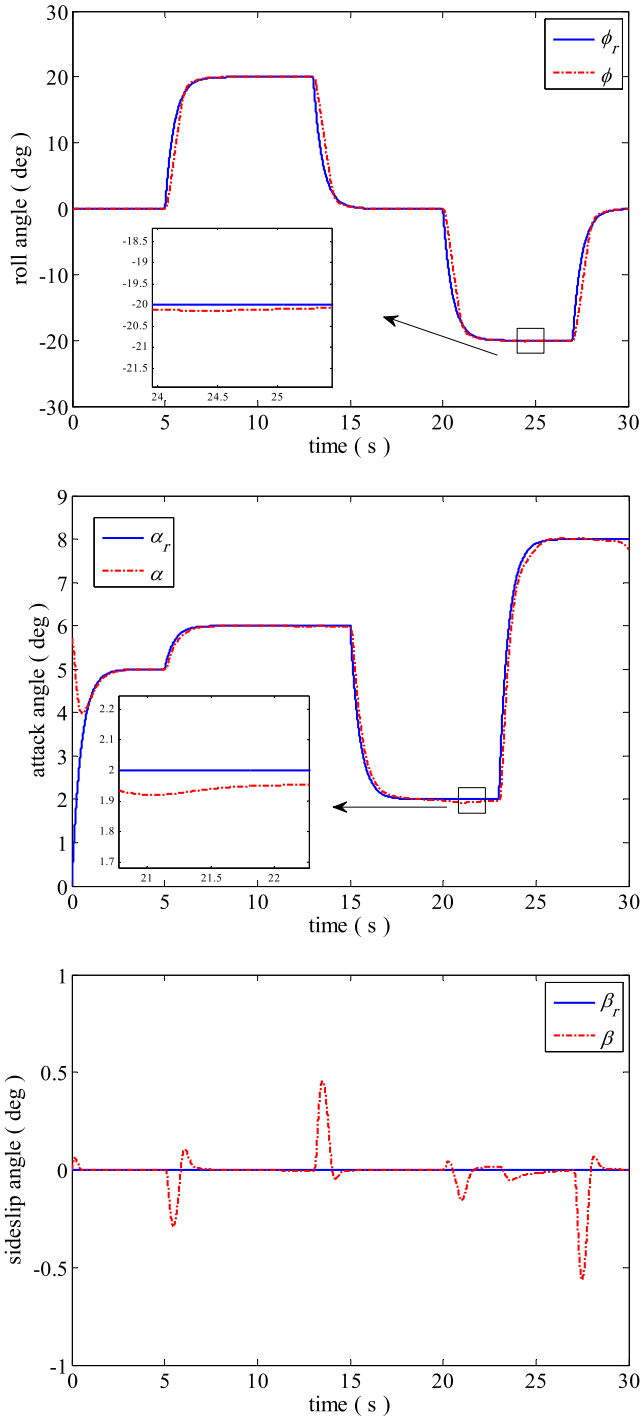

FIGURE 4. Curves of the attitude angles with the constant value $\bar{G}_{inv,i} = diag(0.1, 0.1, 0.1)$.

without knowing the nominal value of the control effectiveness matrix or even under the condition that there are actuator biases and measurement noises, biases, and time delays of the fin deflection angles. Besides, if the appropriate parameters are selected, the tracking errors can converge to a small neighborhood around the origin.

Proof: Please see the controller design process and stability analysis, i.e., (3)-(41).

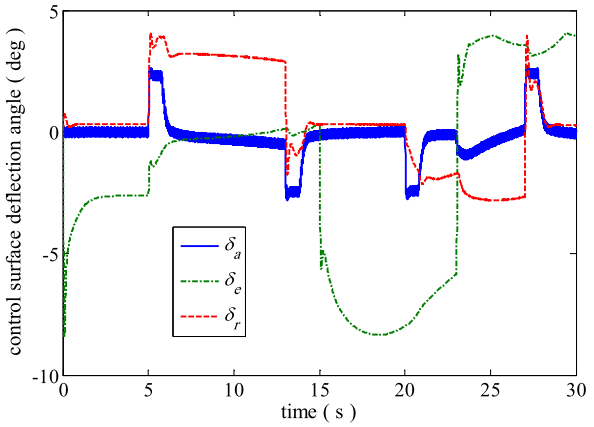

FIGURE 5. Curves of the control surface deflection angles with the constant value $\bar{G}_{inv,i} = diag(0.1, 0.1, 0.1)$.

Remark 5: As for the CFMFR attitude controller for the aircraft, the INDI virtual controller (7) without any information of the function $\boldsymbol{f}_1(\boldsymbol{x}_1)$ is designed for the first subsystem. The elements of control effectiveness matrix $\boldsymbol{g}_1(\boldsymbol{x}_1)$ are functions with respect to the attitude angles, which can be regarded as known functions. In the second subsystem, the TDC method is employed to design the control law (29) where the diagonal matrix with updating laws is used to replace the control effectiveness matrix $\boldsymbol{g}_2(\boldsymbol{x}_1, \boldsymbol{x}_2)$. To sum up, the aerodynamic coefficients and the parameters related to the introduced aircraft are not required to design the control laws. This is why this method is referred to as model free one.

So far, we complete the controller design procedure. Obviously, many signals and parameters are involved in the whole process. Fig. 1 shows the block diagrams of the controller structure, depicting the control process and signal flow according to the actual aircraft control system [17]. The diagram is useful for understanding the signals and relationships among them.

Remark 6: In this paper, we assume the states $\boldsymbol{x}_1 = [\phi\alpha\beta]^{\mathrm{T}}$ and $\boldsymbol{x}_2 = [pqr]^{\mathrm{T}}$ can be measured directly and noises originated from the sensors which are used to measure states $\boldsymbol{x}_1$ and $\boldsymbol{x}_2$ are not taken into consideration. The time derivatives are calculated by the fifth order sliding mode differentiator developed in [39].

IV. SIMULATION STUDY

In this section, a simulation is provided to demonstrate the effectiveness of the developed command filtered model-free robust (CFMFR) control method. Considering the nonlinear 6-DOF model of a flying-wing UAV that was developed primarily in [31] by Guillaume Ducard, we refer to [31] to obtain details regarding the aerodynamic data. The control surfaces consist of an elevator (δ_e), an aileron (δ_a), and a rudder (δ_r). Firstly, we verify the robustness of the approach with actuator biases and measurement errors of the control surface deflection angles. The diagonal matrix is constant here. Besides, two diagonal matrices of the TDC are selected to illustrate that too small elements of the matrix cause poor

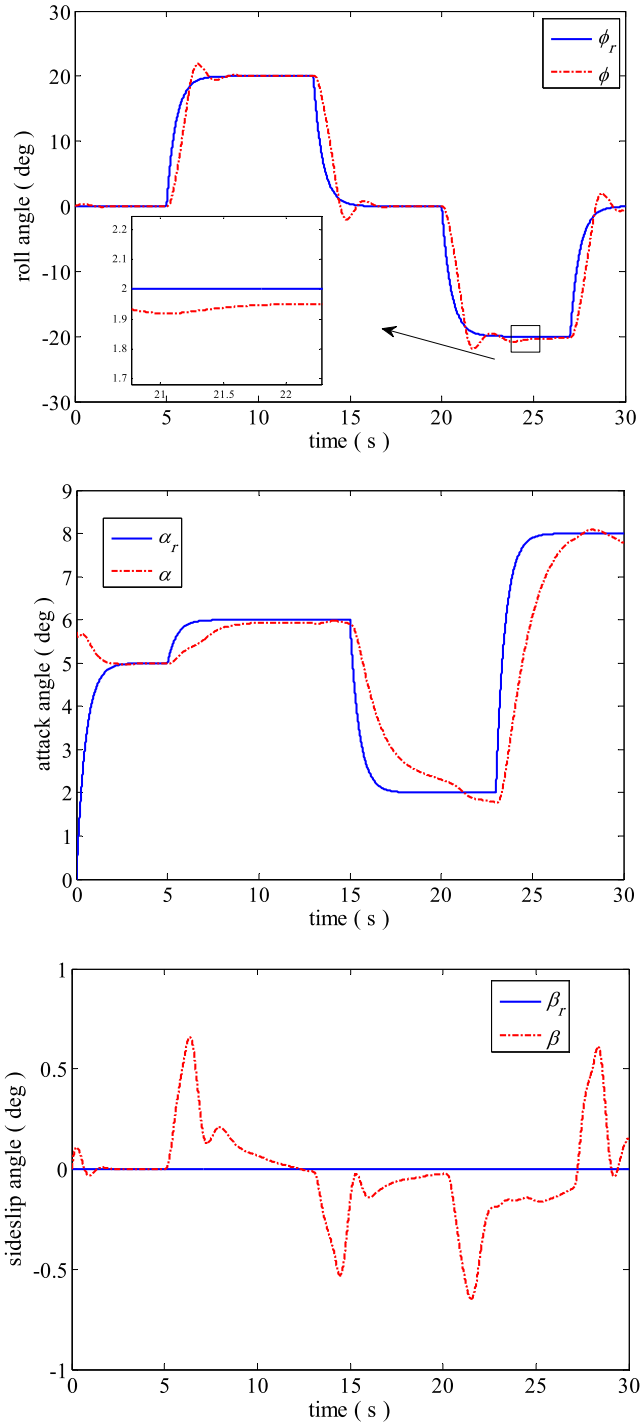

FIGURE 6. Curves of the attitude angles with the constant value $\bar{G}_{inv,i} = diag(0.005, 0.005, 0.005)$.

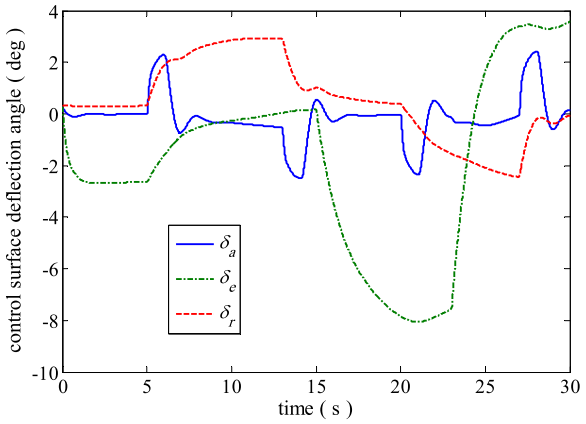

FIGURE 7. Curves of the control surface deflection angles with the constant value $\bar{G}_{inv,i} = diag(0.005, 0.005, 0.005)$.

TABLE 1. Second-order actuator dynamics [40].

Parameter	Unit	Value
Surface deflection limit	deg	–25 to 25
Surface rate limit	deg/s	–100 to 100
Damping ratio ξ	----	0.8
Natural frequency ω_n	rad/s	100

TABLE 2. Command-filter parameters [7].

Command variable	ω_n , rad/s	Mag limit	Rate limit
p	20	±30 deg/s	------
q	20	±20 deg/s	------
r	10	±15 deg/s	------

control performance or even instability of the closed-loop system and too large ones arise chattering of the actuators. At last, we check the effectiveness of the developed CFMFR control method with the updating laws of the elements of the diagonal matrix by adopting different initial values.

The actuator dynamics with the magnitude and rate constraints can be expressed by the introduced second-order command filter. Details regarding the actuator dynamics are presented in Table 1.

We should impose constraints on the virtual control laws through the command filters. The parameters of the command filter are presented in Table 2.

Remark 7: To guarantee the security of the UAVs, we need the variables to vary in the specific zone. In the simulation, the command-filter parameters are designed according to the specific areas of the variables.

To apply the first-order Taylor series expansion and ensure the accuracy of the linearization, the dynamics of the controlled plant must satisfy the TSS property. In the aircraft system, the actuator system can be viewed as a subsystem cascaded to the angular rate dynamic system, so does the angular rate dynamics compared with the attitude angle dynamics. This is largely because the actuator dynamics are faster than the angular rate dynamics. This could be explained as follows. A change in control input of the aircraft has a change in moment as effect. The change in moment is directly effecting the angular accelerations. On the other hand, the angular rates only change by integrating the angular accelerations [41]. Therefore, the TSS property is guaranteed [15].

To illustrate the performance and the robustness to the model errors of the control laws developed herein, the aircraft

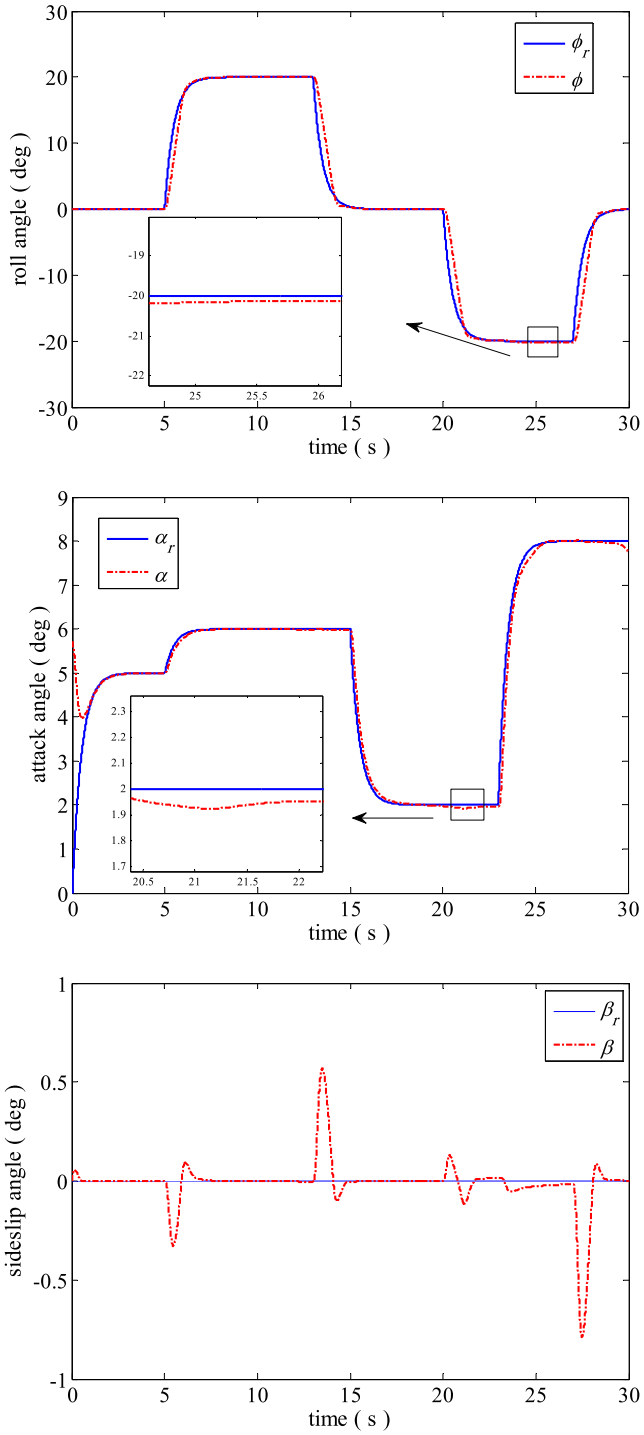

FIGURE 8. Curves of the attitude angles under the action of the proposed CFMFR control method with the initial value $\bar{G}_{inv,i} = diag(0.1, 0.1, 0.1)$.

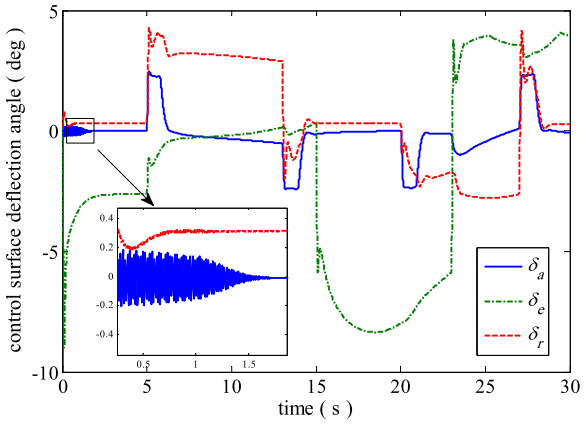

FIGURE 9. Curves of the control surface deflection angles under the action of the proposed CFMFR control method with the initial value $\bar{G}_{inv,i} = diag(0.1, 0.1, 0.1)$.

is commanded to perform doublets in both roll and attack angles simultaneously while regulating the sideslip to zero. This set of the commands is challenging for the autopilot because it includes significant amounts of coupling between all three channels and the modeling errors. In the simulation model, one typical kind of uncertainties, magnitude scaling, is considered. In this case the actual coefficients are obtained by scaling the magnitude of the nominal coefficients. The relations between them can be described as an equation: $C_{*act}(*) = (1 + F_{mag}) C_{*nom}(*)$, where $C_{*act}(*)$ and $C_{*nom}(*)$ are the actual coefficients and nominal coefficients, respectively. $F_{mag} = -30\%$ is the scaling factor [21]. In addition, external disturbances to the aircraft are added. The disturbance of the first subsystem is a constant whose numerical value is diag(30, 30, 30).

In all the simulations, actuator biases and measurement noises, biases and time delays are considered. We assume all the actuator have biases, whose values are $+0.3°$. The independent nonzero mean ($0.2°$) Gaussian noise is added to the measurements with a standard deviation of $+0.1°$. In [17], the simulation results show that the tracking performance is significantly degraded by the oscillation caused by the time delays especially when the value of the time delay is more than $0.2s$. The value of the measurement time delay is $0.3s$.

The design parameters are $k_1 = 4$, $k_2 = 8$, $\lambda = 4$, $\gamma = 1.25$, $\chi = 0.75$, $a_1 = a_2 = a_3 = 20$, $\omega_1 = 0.005$, $\omega_2 = \omega_3 = 0.0005$, $\sigma_1 = \sigma_2 = \sigma_3 = 0.2$.

Firstly, the simulations are conducted with constant gains whose values are $diag(0.05, 0.05, 0.05)$, $diag(0.1, 0.1, 0.1)$, and $diag(0.005, 0.005, 0.005)$, respectively. As shown in Figs. 2-3, the output signals, including the roll angle ϕ, the attack angle α, and the sideslip angle β, can steadily track the given reference signal, and the tracking errors can converge to a small neighborhood around the origin. The chattering performance of the control surfaces are not occurred, from which we can learn that if we can select the right candidate of the constant gain, we can obtain the desired tracking performances. Sometimes, when we select some ill-suited gains, either the chattering phenomenon of the control surfaces are happened or the tracking performances are seriously degraded. As mentioned in Sec.II, as the values of the gains improve, the ultimate tracking errors will be decreased. From the Fig. 4, it is obvious that the tracking errors of the attitude angles of the aircraft can converge to zero or a small neighborhood around the origin. However,

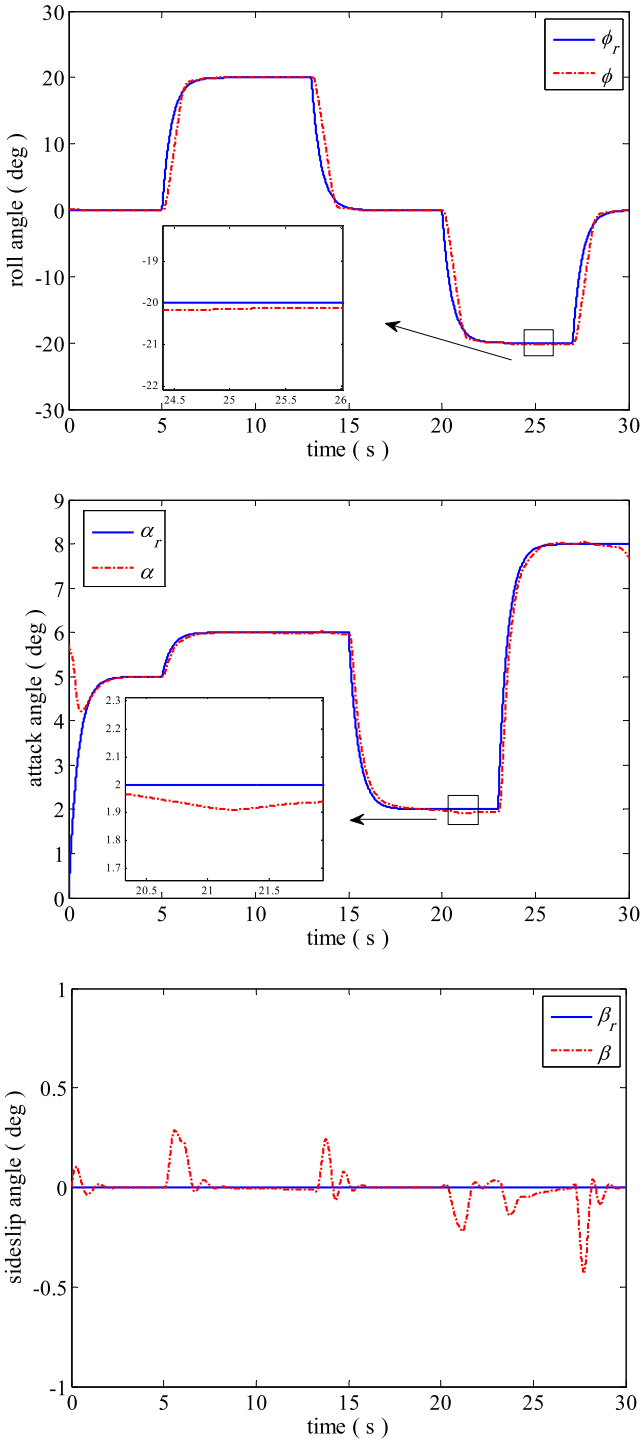

FIGURE 10. Curves of the attitude angles under the action of the proposed CFMFR control method with the initial value $\bar{G}_{inv,i} = diag(0.005, 0.005, 0.005)$.

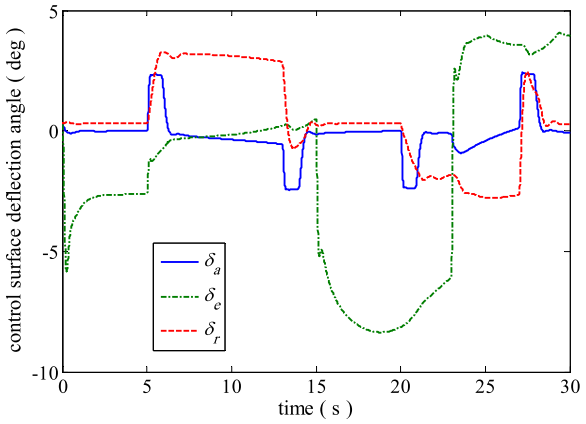

FIGURE 11. Curves of the control surface deflection angles under the action of the proposed CFMFR control method with the initial value $\bar{G}_{inv,i} = diag(0.005, 0.005, 0.005)$.

the actuators, especially δ_a, are chattered, as shown in Fig. 5. Therefore, if we want the flight vehicle to operate steadily and safely, the values of the gains must be reduced. From Fig. 6, we can learn that overshoot of the roll angle and the large tracking errors of the attack angle and the sideslip angle have bad influences on the tracking performances of the vehicle if we let $\bar{G}_{inv,i} = diag(0.005, 0.005, 0.005)$ although the magnitudes and actuating rates of the actuators are kept in the reasonable region (as shown in Fig. 7). Therefore, the values of the gain are vital to the stability of the whole close-loop system. Unfortunately, it's not practical for that lots efforts and time are consumed to select the reasonable constant gain under the circumstances that the nominal value is unknown. So, the adaption scheme should be considered.

In the following simulation experiments, the performances of the CFMFR controller with adaption laws using different initial values of the gain whose values are $diag(0.1, 0.1, 0.1)$ and $diag(0.005, 0.005, 0.005)$, respectively. The Figs. 8-11, especially Figs. 8 and 10, indicate the tracking errors are guaranteed to converge to a small neighborhood around the origin. It can be clearly seen that the developed CFMFR controller with adaption laws can lead to a good tracking performance in the ϕ, α, and β. In Fig. 10, overshoot of the roll angle ϕ is not happened with the help of the adaption laws depending on which the elements of the gain $\bar{G}_{inv}$ are adjusted to obtain the desired tracking performance according to the errors and the values of themselves. As shown in Fig.9, the control surface δ_a is chattered during the time period $t \in [0s, 1.5s]$ when we let the initial value $\bar{G}_{inv,i} = diag(0.1, 0.1, 0.1)$. After that, chattering performance is avoided under the action of the adaption laws designed above. As depicted in Fig. 11, the curves of actuators are similar to Fig. 3 after the parameters are tuned automatically by (30). We also can learn from the Figs. 8-11 that the closed-loop stability can be guaranteed regardless of the selection of the initial values. As long as the initial values are located in the reasonable region (see (28)), the stability would be guaranteed and performance would be improved along with the adaptive laws. The simulation results powerfully verify the effectiveness of the presented CFMFR with adaption laws.

V. CONCLUSION

A command filtered model-free robust (CFMFR) attitude controller is proposed for aircraft with parameter uncertainties and disturbances. The incremental nonlinear dynamic

inversion (INDI) and time-delayed control (TDC) method integrating sliding-mode technique are employed to design the virtual control laws, respectively, according to the reality of the control effectiveness matrix. The updating laws of the diagonal matrix is constructed by Lyapunov control theorem. We considered the actuator dynamics of the control surfaces and the noises, biases, and time delays of the measurements of the control surface deflection angles. The command-filtered backstepping is utilized to compensate the actuator dynamics and filtered errors, and the modified stable linear filter is developed to handle the measurement errors. The stability of the whole closed-loop system, including the compensated signals which are the outputs of the stable linear filters, is analyzed by using Lyapunov theory. Numerical simulation results are performed to demonstrate the chattering of the proposed control method. As for the TDC controller with constant diagonal matrix, instability or fluctuations of the actuators occurs if inappropriate diagonal matrix is chosen. Under the action of the CFMFR controller with auto-tuning diagonal matrix, the high-tracking performance can be obtained regardless of the initial values of the diagonal matrix. In the future work, we will make our control signals optimal or near-optimal by combining reinforcement learning and other machine learning algorithms.

ACKNOWLEDGMENT

X. Li thanks Yongchao Wang, Wei Sun, Naixin. Qi and Yueping Huang for their suggestions.

REFERENCES

[1] I. Kanellakopoulos, P. V. Kokotovic, and A. S. Morse, "Systematic design of adaptive controllers for feedback linearizable systems," *IEEE Trans. Autom. Control*, vol. 36, no. 11, pp. 1241–1253, Nov. 1991.

[2] A. Y. Alanis, E. N. Sanchez, and A. G. Loukianov, "Real-time discrete backstepping neural control for induction motors," *IEEE Trans. Control Syst. Technol.*, vol. 19, no. 2, pp. 359–366, Mar. 2011.

[3] L. Sun, W. Huo, and Z. Jiao, "Adaptive backstepping control of spacecraft rendezvous and proximity operations with input saturation and full-state constraint," *IEEE Trans. Ind. Electron.*, vol. 64, no. 1, pp. 480–492, Jan. 2017.

[4] F. Petit, A. Daasch, and A. Albu-Schäffer, "Backstepping control of variable stiffness robots," *IEEE Trans. Control Syst. Technol.*, vol. 23, no. 6, pp. 2195–2202, Nov. 2015.

[5] D. Swaroop, J. K. Hedrick, P. P. Yip, and J. C. Gerdes, "Dynamic surface control for a class of nonlinear systems," *IEEE Trans. Autom. Control*, vol. 45, no. 10, pp. 1893–1899, Oct. 2000.

[6] J. A. Farrell, M. Polycarpou, M. Sharma, and W. Dong, "Command filtered backstepping," *IEEE Trans. Autom. Control*, vol. 54, no. 6, pp. 1391–1395, Jun. 2009.

[7] J. Farrell, M. Sharma, and M. Polycarpou, "Backstepping-based flight control with adaptive function approximation," *J. Guid. Control Dyn.*, vol. 28, no. 6, pp. 1089–1102, Dec. 2005.

[8] Y. Wang, L. Cao, S. Zhang, X. Hu, and F. Yu, "Command filtered adaptive fuzzy backstepping control method of uncertain non-linear systems," *IET Control Theory Appl.*, vol. 10, no. 10, pp. 1134–1141, Jun. 2016.

[9] H. B. Sun, S. Li, J. Yang, and L. Guo, "Non-linear disturbance observer-based back-stepping control for airbreathing hypersonic vehicles with mismatched disturbances," *IET Control Theory Appl.*, vol. 8, no. 17, pp. 1852–1865, Nov. 2014.

[10] J. Yang, S. Li, C. Sun, and L. Guo, "Nonlinear-disturbance-observer-based robust flight control for airbreathing hypersonic vehicles," *IEEE Trans. Aerosp. Electron. Syst.*, vol. 49, no. 2, pp. 1263–1275, Apr. 2013.

[11] X. Cao, P. Shi, Z. Li, and M. Liu, "Neural-network-based adaptive backstepping control with application to spacecraft attitude regulation," *IEEE Trans. Neural Netw. Learn. Syst.*, vol. 29, no. 9, pp. 4303–4313, Sep. 2018.

[12] S. Sui, S. Tong, and Y. Li, "Adaptive fuzzy backstepping output feedback tracking control of MIMO stochastic pure-feedback nonlinear systems with input saturation," *Fuzzy Sets Syst.*, vol. 254, pp. 26–46, Nov. 2014.

[13] P. Acquatella, W. Falkena, E.-J. van Kampen, and Q. P. Chu, "Robust nonlinear spacecraft attitude control using incremental nonlinear dynamic inversion," in *Proc. AIAA Guid., Navigat., Control (GNC) Conf.*, Minneapolis, MN, USA, Sep. 2012, p. 4623.

[14] P. Lu, E. van Kampen, C. C. de Visser, and Q. P. Chu, "Framework for simultaneous sensor and actuator fault-tolerant flight control," *J. Guid., Control, Dyn.*, vol. 40, no. 8, pp. 2133–2136, Jun. 2017.

[15] L. G. Sun, C. C. de Visser, Q. P. Chu, and J. A. Mulder, "Joint sensor based backstepping for fault-tolerant flight control," *J. Guid., Control, Dyn.*, vol. 38, no. 1, pp. 62–75, Oct. 2014.

[16] L. Cao, Y. Wang, S. Zhang, and T. Fei, "Command-filtered sensor-based backstepping controller for small unmanned aerial vehicles with actuator dynamics," *Int. J. Syst. Sci.*, vol. 49, no. 16, pp. 3365–3376, 2018.

[17] Y. C. Wang, W. S. Chen, S. X. Zhang, J. W. Zhu, and L. J. Cao, "Command-filtered incremental backstepping controller for small unmanned aerial vehicles," *J. Guid., Control, Dyn.*, vol. 41, no. 4, pp. 954–967, Feb. 2018.

[18] L. Sonneveldt, E. R. Van Oort, Q. P. Chu, and J. A. Mulder, "Comparison of inverse optimal and tuning functions designs for adaptive missile control," *J. Guid., Control, Dyn.*, vol. 31, no. 4, pp. 1176–1182, Jul. 2008.

[19] T. Lombaerts, H. Huisman, P. Chu, J. A. Mulder, and D. Joosten, "Nonlinear reconfiguring flight control based on online physical model identification," *J. Guid., Control, Dyn.*, vol. 32, no. 3, pp. 727–748, May 2009.

[20] A. A. H. Ali, Q. P. Chu, E.-J. Van Kampen, and C. C. de Visser, "Exploring adaptive incremental backstepping using immersion and invariance for an F-16 aircraft," in *Proc. AIAA Guid., Navigat., Control (GNC) Conf.*, National Harbor, MD, USA, Jan. 2014, p. 0084.

[21] P. van Gils, E.-J. Van Kampen, C. C. de Visser, and Q. P. Chu, "Adaptive incremental backstepping flight control for a high-performance aircraft with uncertainties," in *Proc. AIAA Guid., Navigat., Control (GNC) Conf.*, San Diego, CA, USA, Jan. 2016, p. 1380.

[22] C. C. de Visser, Q. P. Chu, and J. A. Mulder, "A new approach to linear regression with multivariate splines," *Automatica*, vol. 45, no. 12, pp. 2903–2909, Dec. 2009.

[23] C. C. de Visser, Q. P. Chu, and J. A. Mulder, "Differential constraints for bounded recursive identification with multivariate splines," *Automatica*, vol. 47, no. 9, pp. 2059–2066, Sep. 2011.

[24] L. G. Sun, C. C. de Visser, Q. P. Chu, and J. A. Mulder, "Online aerodynamic model identification using a recursive sequential method for multivariate splines," *J. Guid., Control, Dyn.*, vol. 36, no. 5, pp. 1278–1288, Sep. 2013.

[25] H. J. Tol, C. C. de Visser, L. G. Sun, E. van Kampen, and Q. P. Chu, "Multivariate spline-based adaptive control of high-performance aircraft with aerodynamic uncertainties," *J. Guid., Control, Dyn.*, vol. 39, no. 4, pp. 781–800, Jan. 2016.

[26] K. Youcef-Toumi and S.-T. Wu, "Input/output linearization using time delay control," *J. Dyn. Syst., Meas., Control*, vol. 114, no. 1, pp. 10–19, Mar. 1992.

[27] T. C. Hsia and L. S. Gao, "Robot manipulator control using decentralized linear time-invariant time-delayed joint controllers," in *Proc. IEEE Int. Conf. Robot. Automat.*, Cincinnati, OH, USA, May 1990, pp. 2070–2075.

[28] J. Lee, P. H. Chang, and R. S. Jamisola, "Relative impedance control for dual-arm robots performing asymmetric bimanual tasks," *IEEE Trans. Ind. Electron.*, vol. 61, no. 7, pp. 3786–3796, Jul. 2014.

[29] M. Jin, J. Lee, and N. G. Tsagarakis, "Model-free robust adaptive control of humanoid robots with flexible joints," *IEEE Trans. Ind. Electron.*, vol. 64, no. 2, pp. 1706–1715, Feb. 2017.

[30] D. Chwa, J. Y. Choi, and J. H. Seo, "Compensation of actuator dynamics in nonlinear missile control," *IEEE Trans. Control Syst. Technol.*, vol. 12, no. 4, pp. 620–626, Jul. 2004.

[31] G. J. J. Ducard, *Fault-tolerant Flight Control and Guidance Systems: Practical Methods for Small Unmanned Aerial Vehicles*. London, U.K.: Springer, 2009.

[32] T. Lee and Y. Kim, "Nonlinear adaptive flight control using backstepping and neural networks controller," *J. Guid., Control, Dyn.*, vol. 24, no. 4, pp. 675–682, Jul. 2001.

[33] C.-Y. Li, W.-X. Jing, and C.-S. Gao, "Adaptive backstepping-based flight control system using integral filters," *Aerosp. Sci. Technol.*, vol. 13, nos. 2–3, pp. 105–113, May 2009.

[34] H. K. Khalil, *Nonlinear Systems*, 3rd ed. Upper Saddle River, NJ, USA: Prentice-Hall, 2002.
[35] N. Hovakimyan, E. Lavretsky, and A. Sasane, "Dynamic inversion for nonaffine-in-control systems via time-scale separation. Part I," *J. Dyn. Control Syst.*, vol. 13, no. 4, pp. 451–465, Oct. 2007.
[36] Z. Zhang, Y. Shi, Z. Zhang, and W. Yan, "New results on sliding-mode control for takagi–sugeno fuzzy multiagent systems," *IEEE Trans. Cybern.*, vol. 49, no. 5, pp. 1592–1604, May 2019.
[37] A.-M. Zou, Z.-G. Hou, and M. Tan, "Adaptive control of a class of nonlinear pure-feedback systems using fuzzy backstepping approach," *IEEE Trans. Fuzzy Syst.*, vol. 16, no. 4, pp. 886–897, Aug. 2008.
[38] E. Kim and S. Lee, "Output feedback tracking control of MIMO systems using a fuzzy disturbance observer and its application to the speed control of a PM synchronous motor," *IEEE Trans. Fuzzy Syst.*, vol. 13, no. 6, pp. 725–741, Dec. 2005.
[39] A. Levant, "Higher-order sliding modes, differentiation and output-feedback control," *Int. J. Control*, vol. 76, nos. 9–10, pp. 924–941, Jan. 2003.
[40] D. P. Wiese, A. M. Annaswamy, J. A. Muse, M. A. Bolender, and E. Lavretsky, "Adaptive output feedback based on closed-loop reference models for hypersonic vehicles," *J. Guid., Control, Dyn.*, vol. 38, no. 12, pp. 2429–2440, May 2015.
[41] S. Sieberling, Q. P. Chu, and J. A. Mulder, "Robust flight control using incremental nonlinear dynamic inversion and angular acceleration prediction," *J. Guid., Control, Dyn.*, vol. 33, pp. 1732–1742, Jun. 2010.

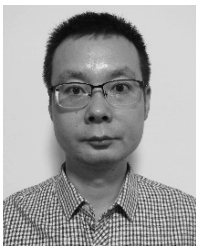

XIAOFENG LI received the B.S., M.S., and Ph.D. degrees from the Xi'an Research Institute of Hi-Tech, Xi'an, China, in 2005, 2008, and 2012, respectively, where he is currently a Lecturer. His research interests include guidance and control of aircrafts.

LIJIA CAO received the B.S., M.S., and Ph.D. degrees from the Xi'an Research Institute of Hi-Tech, Xi'an, China, in 2005, 2008, and 2012, respectively. He is currently an Associate Professor with the Sichuan University of Science and Engineering, the Artificial Intelligence Key Laboratory of Sichuan Province, and the Sichuan Key Provincial Research Base of Intelligent Tourism. His main research interests include guidance and control of UAVs.

XIAOXIANG HU received the B.S., M.S., and Ph.D. degrees from the Xi'an Research Institute of Hi-Tech, Xi'an, China, in 2005, 2008, and 2012, respectively. He is currently an Associate Professor with the School of Automation, Northwestern Polytechnical University. His current research interests include fuzzy control, sliding mode control, and hypersonic fight vehicles.

SHENGXIU ZHANG received the Ph.D. degree from the School of Electronic and Information Engineering, Xi'an Jiaotong University, Xi'an, China, in 2001. He is currently a Professor with the Xi'an Research Institute of Hi-Tech. His main research interests include adaptive control, guidance, navigation, and control of the aircrafts to optimal control for UAVs.